

# The Statistics of Oceanic Turbulence Measurements. Part II: Shear Spectra and a New Spectral Model

ROLF G. LUECK<sup>a</sup>

<sup>a</sup> *Rockland Scientific, Inc., Victoria, British Columbia, Canada*

(Manuscript received 1 February 2021, in final form 31 March 2022)

**ABSTRACT:** This manuscript provides (i) the statistical uncertainty of a shear spectrum and (ii) a new universal shear spectrum, and (iii) shows how these are combined to quantify the quality of a shear spectrum. The data from four collocated shear probes, described in Part I, are used to estimate the spectra of shear,  $\Psi(k)$ , for wavenumbers  $k \geq 2$  cpm, from data lengths of 1.0 to 50.5 m, using Fourier transform (FT) segments of 0.5 m length. The differences of the logarithm of pairs of simultaneous shear spectra are stationary, distributed normally, independent of the rate of dissipation, and only weakly dependent on wavenumber. The variance of the logarithm of an individual spectrum,  $\sigma_{\ln\Psi}^2$ , equals one-half of the variance of these differences and is  $\sigma_{\ln\Psi}^2 = 1.25N_f^{-7/9}$ , where  $N_f$  is the number of FT segments used to estimate the spectrum. This term  $\sigma_{\ln\Psi}$  provides the statistical basis for constructing the confidence interval of the logarithm of a spectrum, and thus, the spectrum itself. A universal spectrum of turbulence shear is derived from the nondimensionalization of 14 600 spectra estimated from 5 m segments of data. This spectrum differs from the Nasmyth spectrum and from the spectrum of Panchev and Kesich by 8% near its peak, and is approximated to within 1% by a new analytic equation. The difference between the logarithms of a measured and a universal spectrum, together with the confidence interval of a spectrum, provides the statistical basis for quantifying the quality of a measured shear (and velocity) spectrum, and the quality of a dissipation estimate that is derived from the spectrum.

**SIGNIFICANCE STATEMENT:** The results reported here can be used to estimate the statistical uncertainty of a spectrum of turbulent shear or velocity that is derived from a finite number of discrete Fourier transform segments, and they can be used to quantify the quality of a spectrum.

**KEYWORDS:** Data quality control; In situ oceanic observations; Measurements

## 1. Introduction

This paper is Part II of a two-part series dealing with the statistical uncertainty of turbulence shear measurements. Lueck (2022, hereafter [Part I](#)) presented data collected from four collocated shear probes positioned 15 m above the bottom in a tidal channel. For an 18.5 km long subset of these data, dissipation rates were small enough ( $\leq 10^{-5}$  W kg<sup>-1</sup>) for the shear probes to fully resolve the shear variance, and currents were weak enough ( $\leq 1$  m s<sup>-1</sup>) to keep platform vibrations small relative to the turbulence shear. These data were processed to produce a space series of shear, which is nearly free of anomalous signals, and the variance of this shear signal (and hence, the rate of dissipation) was estimated directly in the space domain, using the first equality in (1).

Because the separation of the probes is small ( $\leq 0.05$  m) compared to the distance to the bottom, the variances of shear derived from each of the four probes agree closely on average, even when successive estimates change by several factors of 10. The disagreement among the probes is due to the statistical nature of the turbulence shear and its limited sampling. The differences of the logarithm of the rate of


dissipation estimated from the probes are distributed normally. The variance of the measurement from an individual probe equals one-half of the variance of these differences and is  $\sigma_{\ln\epsilon}^2 \approx 16\hat{L}^{-7/9}$ , for  $\hat{L} \gg 4$ , where  $\hat{L} = L/L_K$ ,  $L$  is the averaging length, and  $L_K = (\nu^3/\epsilon)^{1/4}$  is the Kolmogorov length.

It is seldom possible to estimate the rate of dissipation directly from the variance of shear (as was done in [Part I](#)) because of electronic noise and spurious content in a shear-probe signal. Instead, the variance of shear is usually estimated from its spectrum. In isotropic turbulence ([Taylor 1935](#); [Pope 2009](#)) the rate of dissipation is given by

$$\epsilon = \frac{15}{2} \overline{\left(\frac{\partial w}{\partial x}\right)^2} = \frac{15}{2} \nu \int_0^\infty \Psi(k) dk \approx \frac{15}{2} \nu \int_0^{k_u} \Psi(k) dk, \quad (1)$$

where  $\nu$  is the kinematic viscosity,  $w$  is any velocity component orthogonal to the direction of profiling,  $x$  is any direction of profiling,  $\Psi(k)$  is the spectrum of shear,  $k$  is the wavenumber in the  $x$  direction, and  $k_u < \infty$  is an upper wavenumber imposed by practical considerations, such as the avoidance of noise and vibrational contamination in the shear-probe signal.

This paper (Part II) will use the space series of shear developed in [Part I](#) to derive the statistical uncertainty of a spectrum using the same notion that the spectra from the four probes should agree, on average. The analysis will show that the differences of the logarithm of the spectra are independent of the rate of dissipation and of wavenumber, and that these differences are due to the statistical nature of a shear

 Denotes content that is immediately available upon publication as open access.

Corresponding author: Rolf Lueck, [rolf@rocklandscientific.com](mailto:rolf@rocklandscientific.com)

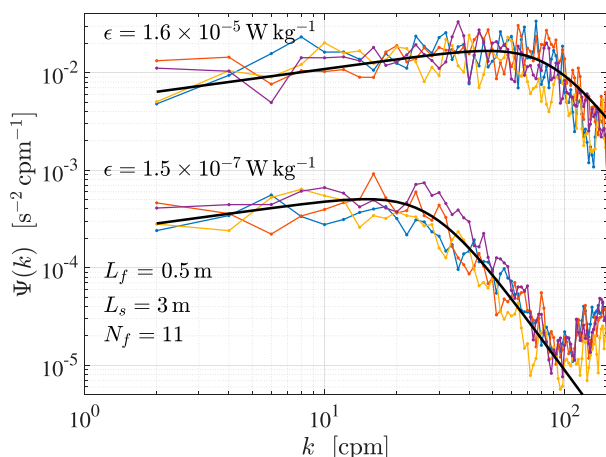


FIG. 1. Two examples of spectra from four collocated shear probes using 3 m of data (colored curves). The upper (lower) set come from a region of high (low) dissipation rates, which are indicated above each set. The black lines are the Nasmyth dimensional spectra for the indicated  $\epsilon$  values. The spectra were computed using  $N_f = 11$  FT segments of 0.5 m length, a cosine taper, and an overlap of 50%.

spectrum and the limited data used to estimate the spectrum, which is evident in Fig. 1.

A quantitative assessment of the quality of a spectrum requires knowledge of the statistical uncertainty of the spectrum (its confidence interval) and a model of the expectation of the spectrum. The expectation spectrum is only known empirically from observations (Nasmyth 1970; Oakey 1982; Pope 2009; Roget et al. 2006; Panchev and Kesich 1969). The very large volume of data derived in Part I will also be used to make a new estimate of the universal (nondimensional) spectrum of shear and this estimate will be compared against the existing empirical models.

This article is structured as follows. Section 2 describes the spectral estimation method. Section 3 presents the pdf of the differences of the logarithm of the spectral estimates, for a wide range of data lengths, and describes the application of the derived pdf to the confidence interval of a spectrum. In section 4a approximately 14 600 spectra are nondimensionalized and bin averaged to provide another estimate of the universal (nondimensional) shear spectrum. The Nasmyth spectrum of shear is reexamined in section 4b to provide a new approximation that preserves its integral properties. The bin-averaged spectrum is compared against the spectrum of Nasmyth and that of Panchev–Kesich in section 4c. A simulation is used in section 5 to show that the dependence of the spectral uncertainty on the number of FT segments used to estimate a spectrum is a natural consequence of the lognormal pdf of a shear spectrum, and that the uncertainty of an  $\epsilon$  estimate made by spectral integration is identical to the estimate made directly from the variance of shear in Part I. In addition, this section shows how a spectrum, its expectation, and its confidence interval can be used to quantify the quality of a spectrum. The results are concluded in section 6.

## 2. Spectral estimation

### a. Spectral uncertainty

To derive the statistical uncertainty of a spectral estimate, spectra were calculated with the periodogram method, using data lengths of  $L_s = 1$  to 50.5 m, and FT segments of length  $L_f = 0.5$  m. The FT segments were overlapped by 50% and tapered with a cosine window. The number of FT segments used to estimate each spectrum is  $N_f = 2L_s/L_f - 1$  and ranged from 3 to 100. The wavenumber spacing of the spectral values is 2 cpm. The vibration-coherent noise removal algorithm of Goodman et al. (2006) is not applied because many of the spectral estimates are too short ( $N_f$  is too small) for a reliable estimate of the coherency between the vibration and the shear-probe signals. The FT-segment length was chosen to be 0.5 m to maximize the number of spectra that can be calculated, while keeping small the variance located below the lowest non-zero wavenumber (of 2 cpm).

### b. Nondimensional spectra

For the estimation of the nondimensional shear spectrum, as opposed to its uncertainty, a uniform data length  $L_s = 5$  m is chosen, corresponding to about 5000 Kolmogorov lengths. This provides a 95% confidence interval of [0.75, 1.33] for the  $\epsilon$  estimates which are required for nondimensionalizing the shear spectrum. In addition, with  $N_f = 19$  segments of 0.5 m length, the estimates of coherency are reliable enough for using the vibration-coherent noise removal algorithm of Goodman et al. (2006).

The upper limit of spectral integration,  $k_u$ , is determined from the minimum of a third-order polynomial that is fitted to the spectrum in log–log space. The spectra are dominated by electronic noise for wavenumbers larger than this minimum. There is no spectral minimum when dissipation rates are high. The spectra are integrated to the spectral minimum, or maximum of 150 cpm when there is no minimum, using the trapezoidal method. The rate of dissipation is then derived using the approximation in (1). The fraction of the shear variance that is excluded by spectral truncation at  $k_u$  is estimated from a model of the Nasmyth spectrum, and this correction is typically 5%.

The example of a low dissipation spectrum (Fig. 1, lower set) shows a spectrum with a high-wavenumber minimum at 90 cpm, and electronic noise rising at higher wavenumbers. The variance is 95% resolved at this wavenumber. The example of a high dissipation spectrum (upper set) does not have a minimum because the signal is much larger than the electronic noise, and the integration is terminated at 150 cpm where the spectrum is 90% resolved.

## 3. Statistics of spectrum differences

Let the spectra estimated by the method of section 2a be denoted by

$$\Psi_i^{N_f}(k), \quad (2)$$

where the subscripted index,  $i = 1, \dots, 4$ , represents the probe number. Probes 1 and 3 measure the shear of vertical velocity,

while 2 and 4 sense the shear of lateral velocity (Part I, Fig. 1b). The superscript  $N_f$  identifies the number of FT segments used to estimate the spectrum.

As shown in Part I for  $\epsilon$  estimates, if the spectrum of the shear of one component of velocity,  $\Psi_i^{N_f}(k)$ , is distributed log-normally, then the ratio of two spectra of orthogonal components,  $Z = \Psi_i^{N_f}/\Psi_j^{N_f}$ , is also distributed log-normally. If the turbulence is isotropic, then the mean of the logarithm of the ratio is  $\mu_z = 0$  and the variance of the ratio is  $\sigma_z^2 = 2\sigma_i^2$ , where  $\sigma_i^2$  is the variance of the logarithm of either spectrum that was estimated using  $N_f$  FT segments.

The spectra of the four simultaneously measured shear signals are used to form the spectral differences

$$\Delta_{ij}^\Psi(N_f, k) = \ln[\Psi_i^{N_f}(k)] - \ln[\Psi_j^{N_f}(k)] \quad (3)$$

for the  $i, j$  pairs of (1,2), (1,4), (2,3), and (3,4). These  $i, j$  pairs represent orthogonal probes that are nearly statistically independent and form unbiased estimates of their logarithmic differences (Part I). Probe pairs that measure the same component of shear are not used because they are partially interdependent for wavenumbers smaller than 10 cpm, which biases low the difference of the logarithm of their spectra. The notion is that these spectral differences should depend only on  $N_f$ , and be independent of the levels of the spectra (and dissipation rate) in the wavenumber range that excludes electronic noise.

The skew of the differences is estimated using

$$S = \frac{1}{M}[\Delta^\Psi(N_f)]^3, \quad (4)$$

where  $M$  is the total number of spectral differences, and  $\Delta^\Psi$  is the ensemble of spectral difference (3) using all  $i, j$  pairs, and all wavenumbers  $k \leq 0.8 k_u$ . The wavenumber range is curtailed to avoid bias from electronic noise near  $k_u$ . The kurtosis is estimated using

$$K = \frac{1}{M}[\Delta^\Psi(N_f)]^4 - 3. \quad (5)$$

For the segment extracted from file MP2\_096 and  $N_f = 6$ , the standard deviation of the spectral differences for all wavenumbers,  $k \leq 120$  cpm, does not depend on position within this segment (Fig. 2a). The standard deviation of all probe pairs and all wavenumbers does not depend on the rate of dissipation,  $\epsilon$  (Fig. 2b). However, the standard deviations of the differences are slightly wavenumber dependent (Fig. 2c) with a maximum in the 80 to 100 cpm range. This range is near to the peak of the shear spectrum at high dissipation rates,  $\epsilon \sim 10^{-5} \text{ W kg}^{-1}$ , and near to the electronic noise floor for low dissipation rates,  $\epsilon \sim 10^{-7} \text{ W kg}^{-1}$  (Fig. 1). Since the rise of the standard deviation with increasing wavenumber is systematic above 20 cpm, regardless of the spectral level (dissipation rate), it is likely unrelated to electronic noise.

The differences of the logarithm of the spectra from all four probe pairs and all wavenumbers  $k \leq 120$  cpm, using the data extracted from file MP2\_096, are close to normal (Fig. 3). The standard deviation of the spectral differences decreases with

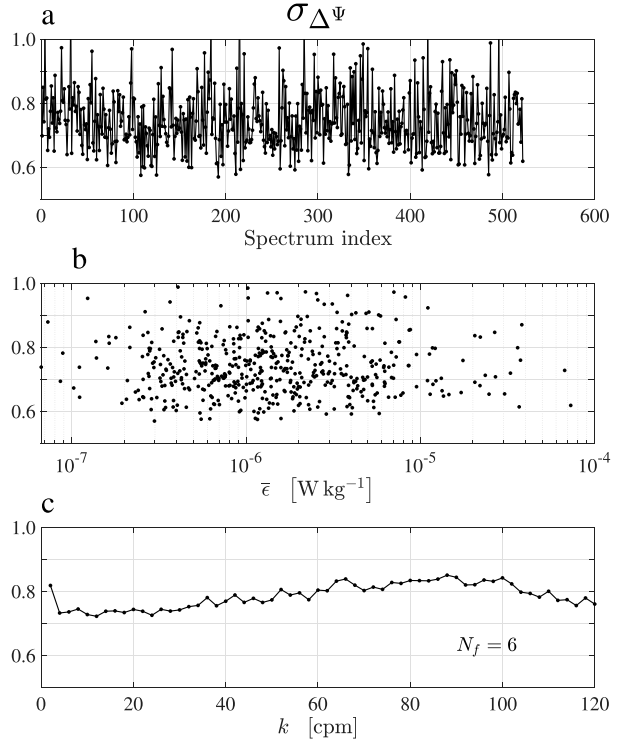


FIG. 2. The standard deviation of the difference of the logarithm of the spectra from probe pairs as a function of (a) position within a 915 m segment, (b) the rate of dissipation derived from each spectrum, and (c) the wavenumber of the spectra. This segment yielded 522 spectra, from each probe, using  $N_f = 6$  FT segments of length 0.5 m.

increasing number of FT segments,  $N_f$ , that are used to form a spectrum. The pdfs are slightly skewed (typically by less than 0.1) and their kurtosis is positive and smaller than 0.25. Samples outside of the range of  $\pm 4$  standard deviations were excluded from the estimation of the sample skew and kurtosis. Including extreme values doubles both statistics.

The degrees of freedom of the spectral differences is

$$d_f = \frac{1}{2} \left( \frac{3.9}{4} \right) N_s N_k, \quad (6)$$

where  $N_s$  is the number of spectra that can be computed for a given  $N_f$ ,  $N_k$  is the number of wavenumber points in a spectrum, the factor in braces accounts for the slight interdependence of the probe-pair differences, and the factor of 1/2 accounts for the interdependence of adjacent spectral values due to applying a cosine window to each FT segment. The number of spectral points,  $N_k$ , varies among the data segments that were extracted and equals the number of wavenumber values that are smaller than 80% of the cutoff wavenumber  $k_u$  or approximately 70 (see Part I, Table 2).

Quantile–quantile, q–q, plots (not shown) of the cumulative density function pass the Kolmogorov–Smirnov (KS) test at the 5% level of significance for nearly every value of  $N_f$ . There is a small failure for about one-half of the samples for

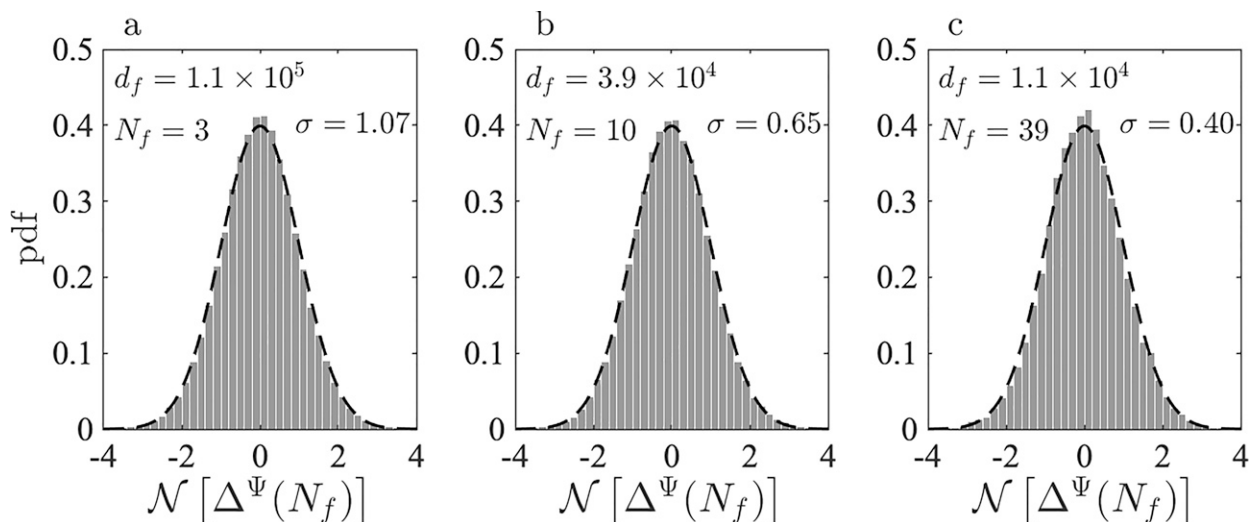


FIG. 3. The pdfs of the spectral differences (3) using all four probe pairs for a 915 m segment extracted from a single file for the case of FT segments of  $N_f =$  (a) 3, (b) 10, and (c) 39 (gray bars). Each group is normalized by its standard deviation  $\sigma$  and they all conform closely to a standard normal distribution (dashed line);  $d_f$  is the degrees of freedom.

$N_f = 3$ . Fewer than 1% of the samples fail the KS test for  $N_f \geq 10$ .

The spectral differences (3) have been calculated, using all of the extracted file segments, all orthogonal probe pairs, and all wavenumbers smaller than  $0.8k_u$ , to estimate the variance of a spectrum of shear due to using a finite number of FT segments,  $N_f$ , namely,

$$\sigma_{\ln \Psi}^2 = \frac{1}{2} \text{Var}(\Delta \Psi). \quad (7)$$

This is the measurement variance due to the statistical nature of turbulent shear, and has been calculated for  $N_f$  ranging from 3 to 100 to determine its dependence on  $N_f$  (Fig. 4, disks). There is segment-to-segment variability, but the 95% bootstrap confidence interval for the mean at each  $N_f$  is very small (dark gray shading). The mean variance is approximated by

$$\sigma_{\ln \Psi}^2 = \frac{5}{4} N_f^{-7/9} + 0.015 \approx \frac{5}{4} N_f^{-7/9} \quad (8)$$

(Fig. 4, solid line). The same analysis for the data collected in the thermocline over Faroe Bank Channel (Fer et al. 2014) produces estimates of the measurement variance (triangles) that are slightly larger than those obtained from the Minas Passage data. However, the Faroe Bank data are limited (4000 m of data and only a single probe pair) and their 95% bootstrap confidence interval for  $\sigma_{\ln \Psi}^2$  is comparatively large (Fig. 4, light gray shading) and overlaps the Minas Passage estimates.

The offset in (8) is peculiar because the expectation is a variance that decreases to zero with increasing  $N_f$ . The electronic voltage noise in each probe signal is nearly identical and, so, the difference of this noise variance should also vanish for large  $N_f$ . However, the probes do not have identical sensitivities and the

electronic noise, expressed in terms of shear, is not identical among the probe signals. For arbitrarily large  $N_f$  the variance of the differences reflects the difference in the electronic noise variance (in terms of shear) among the probe pairs, and this variance approaches a constant at large  $N_f$ . The constant in (8) is only important for  $N_f > 100$  and can, thus, be ignored for lower (and more typical)  $N_f$  values.

### Application

The empirical model of the standard deviation of a spectral estimate (8) can be used to place a confidence interval on a

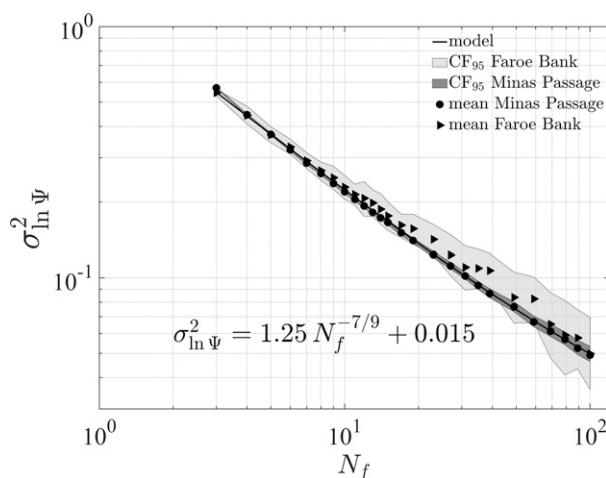


FIG. 4. The mean variance of the measurement error,  $\sigma_{\ln \Psi}^2$ , (7), as a function of the number of FT segments,  $N_f$ , used to estimate a spectrum. Disks and dark gray shading: Minas Passage mean variance and its 95% confidence interval. Triangles and light gray shading: same using Faroe Bank Channel data. Line: approximation of (8).

spectrum that uses a finite number of FT segments,  $N_f$ . The 95% confidence interval of the logarithm of a shear spectrum estimate  $\Psi$  is  $\pm 1.96\sigma_{\ln\Psi}$ , and therefore, there is a 95% probability that the logarithm of the true spectral valued  $\bar{\Psi}$  is in the range of

$$\ln\bar{\Psi} = \ln\Psi \pm 1.96\sigma_{\ln\Psi}. \quad (9)$$

Thus, the confidence interval of  $\bar{\Psi}$  is

$$\text{CI}_{95}(\bar{\Psi}) = \bar{\Psi} \exp(\pm 1.96\sigma_{\ln\Psi}). \quad (10)$$

The factor of 1.96 can be adjusted for other confidence intervals.

If two or more probes are used simultaneously to measure a shear spectrum, then a test for agreement among the probes is the confidence interval

$$\text{CI}_{95}(\Psi_p) = \bar{\Psi}_p \exp\left(\pm 1.96 \frac{p-1}{p} \sigma_{\ln\Psi}\right), \quad (11)$$

where  $\bar{\Psi}_p$  is the average of the  $p$  spectra and  $\Psi_p$  is the spectrum from any one of the  $p$  probes. That is, 95% of the spectral values from each probe should be within this interval. The confidence interval is tighter, compared to (10), by the factor  $(p-1)/p$  because one degree of freedom is consumed in estimating the average spectrum. Logarithmic differences of more than  $\pm 4\sigma_{\ln\Psi}$  should be treated with suspicion. However, these confidence limits are relative. They apply to a comparison of two or more simultaneously measured spectra from collocated probes. An absolute determination of the quality of a spectrum requires comparing it to an expectation spectrum, with due regard for the confidence limits of a spectrum. An expectation spectrum is derived next.

#### 4. The turbulence shear spectrum

##### a. Nondimensional shear spectrum

The 18.5 km data are used to construct approximately 14600 spectra,  $\Psi_D$ , and an equal number of dissipation estimates  $\epsilon$ , by the method described in section 2b. These spectra, each derived from 5 m of data, are nondimensionalized using

$$\Psi(\hat{k}) = \frac{L_K^2}{(\epsilon\nu^5)^{1/4}} \Psi_D(k) \quad (12)$$

$$\hat{k} = kL_K, \quad L_K = (\nu^3/\epsilon)^{1/4},$$

where the kinematic viscosity  $\nu$  is nearly constant at  $1.1 \times 10^{-6} \text{ m}^2 \text{ s}^{-1}$ , because the temperature varied by less than a degree from  $17^\circ\text{C}$ . The nondimensional cyclic wavenumbers,  $\hat{k}$ , are different for every spectrum (Fig. 5, gray dots). The spectra have been averaged into 20 bins that are uniformly centered, in logarithmic space, over wavenumbers ranging from  $2 \times 10^{-3}$  to 0.1 (solid disks). The lower edge of the first bin is at  $1.7 \times 10^{-3}$  and the upper edge of the last bin is at 0.13.

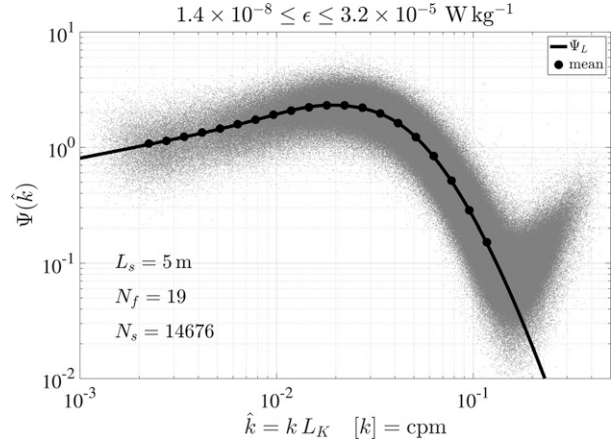


FIG. 5. The 14676 spectra of shear, nondimensionalized using (12) (gray dots), the new approximation of (13) (line), and the bin averages of the spectral values (disks) using data from Minas Passage. The range of  $\epsilon$  is given at the top.

An approximation of the bin-averaged spectrum is

$$\Psi_L(\hat{k}) = \frac{8.048\hat{k}^{1/3}}{1 + (21.7\hat{k})^3} \left[ \frac{1}{1 + (6.6\hat{k})^{5/2}} \left[ 1 + \frac{0.36y}{(y-1)^2 + 2y} \right] \right] \quad (13)$$

$$y = \left( \frac{\hat{k}}{0.015} \right)^2.$$

It has a Kolmogorov constant of 0.52. The compensated spectrum,  $\hat{k}^{-1/3}\Psi_L(\hat{k})/8.048$ , is level at a value of 1 for low wavenumbers, but it rises to a peak of 1.14 at a cyclic nondimensional wavenumber of 0.013. The very high Reynolds number wind tunnel observations of Saddoughi and Veeravalli (1994) have peaks in the compensated shear spectrum of 1.08 at the same wavenumber of 0.013. This approximation has an asymptotic rolloff that is proportional to  $\hat{k}^{-31/6}$ , and does not have the exponential rolloff predicted by Kraichnan (1959) and observed by Saddoughi and Veeravalli (1994) among others.

##### b. Other empirical approximations

###### 1) THE NASMYTH EMPIRICAL MODEL

A frequently used reference spectrum is that of Nasmyth (1970, hereafter PN), who provided a graphic illustration of the nondimensional along-profile velocity spectrum. Fifteen values of this spectrum, spaced fairly uniformly with respect to the logarithm of wavenumber, were tabulated by Oakey (1982, hereafter NO). PN did not measure shear. His data were collected with a towed vehicle in a highly turbulent tidal channel using a conical hot-film probe (Grant et al. 1962) that measures along-profile velocity fluctuations. In isotropic turbulence, the spectrum of the along-profile velocity fluctuations  $E_{11}(\kappa)$  is nondimensionalized using

$$E_{11}(\kappa) = (\epsilon\nu^5)^{1/4} F_{11}(\hat{\kappa}) \quad (14)$$

$$\hat{\kappa} = \kappa \left( \frac{\nu^3}{\epsilon} \right)^{1/4},$$



where  $\kappa$  is the angular wavenumber in the direction of the profile and has units of  $\text{rad m}^{-1}$ ,  $\hat{\kappa}$  is the nondimensional angular wavenumber derived using the Kolmogorov length  $L_K = (\nu^3/\epsilon)^{1/4}$  (Pope 2009).  $F_{11}$  is expected to be a universal function independent of the rate of dissipation and the molecular viscosity. In the inertial subrange,  $F_{11}$  is proportional to  $\hat{\kappa}^{-5/3}$  (Kolmogorov 1941) but there is no satisfactory theory for its form at higher wavenumbers, except that it is ultimately proportional to  $\exp(-\beta\hat{\kappa})$  (Kraichnan 1959), where  $\beta \approx 5.2$  (Pope 2009). The values of  $F_{11}$  derived by PN are tabulated in NO for nondimensional cyclic wavenumbers,  $\hat{k} = k L_K$ , from  $2.83 \times 10^{-4}$  to 0.252, with five values per decade (approximately). The cyclic wavenumber  $k$  is smaller than the angular wavenumber  $\kappa$  by a factor of  $2\pi$ .

The spectrum of across-profile velocity fluctuations,  $E_{22}(\kappa)$ , is nondimensionalized by

$$E_{22}(\kappa) = (\epsilon\nu^5)^{1/4} F_{22}(\hat{\kappa}), \quad (15)$$

where  $F_{22}$  is another universal function, that is related to the along-profile velocity spectrum through

$$F_{22}(\hat{\kappa}) = \frac{1}{2} \left( 1 - \hat{\kappa} \frac{d}{d\hat{\kappa}} \right) F_{11}(\hat{\kappa}) \quad (16)$$

(Pope 2009). NO fitted a parabola to each of the 13 triplets of adjacent spectral values, in log-log space, and used these second-order curves to estimate the slope of  $F_{11}$  in linear space for all 15 spectral points. He estimated  $F_{22}$  using 16 and the Nasmyth shear spectrum using  $\hat{\kappa}^2 F_{22}$ .

Two characteristics of isotropic turbulence that are implicit in a velocity spectrum were not addressed by NO—(i) the Kolmogorov constant is implicitly represented by the level of the spectrum in the inertial subrange (the  $\hat{\kappa}^{-5/3}$  range) and (ii) the integrals of the rate of strain spectrum  $\hat{\kappa}^2 F_{11}$  and the shear spectrum  $\hat{\kappa}^2 F_{22}$  must equal  $1/15$  and  $2/15$ , respectively. The Kolmogorov constant implied in the Nasmyth values for  $F_{11}$  is 0.52, which places it within the range of 0.51 to 0.55 suggested by Sreenivasan (1995).

The spectral values of  $F_{11}$  are too coarsely spaced to estimate the integral of  $\hat{\kappa}^2 F_{11}$  directly using the trapezoidal method of integration. A cubic spline approximation, using 6795 points, yields an integral that is 2% larger than  $1/15$ . To maintain consistency with the integral requirement of  $\hat{\kappa}^2 F_{11}$ , while also retaining the shape of  $F_{11}$ , I have reduced the values of  $F_{11}$ , reported by NO, by 2%. This reduces the Kolmogorov constant to 0.51 and places it at the bottom of the Sreenivasan (1995) range. Consequently, the shear spectrum tabulated by NO is also reduced by 2% to preserve its integral property (Fig. 6, square markers).

An analytic approximation to the (2% reduced) Nasmyth shear spectrum is

$$\Psi_N(\hat{k}) = \frac{7.89 \hat{k}^{1/3}}{1 + (21.2 \hat{k})^3} \left[ \frac{1}{1 + (6 \hat{k})^{5/2}} \right] \left[ 1 + \frac{0.11 y}{(y - 1)^2 + y/2} \right] \quad (17)$$

$$y = \left( \frac{\hat{k}}{0.019} \right)^2,$$

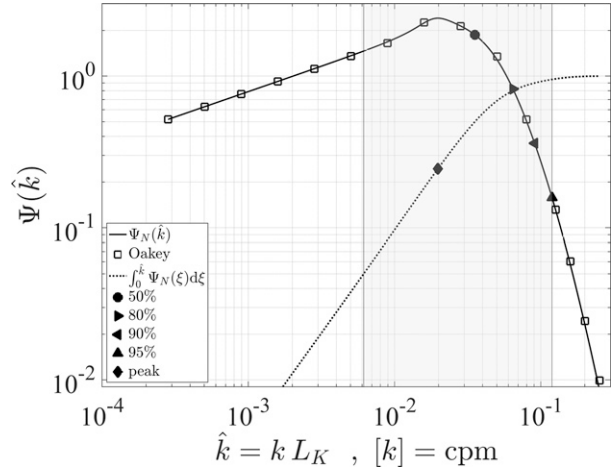


FIG. 6. The Nasmyth spectral shear values, reduced by 2% from the values reported by NO, as a function of the cyclic wavenumber  $\hat{k}$ , nondimensionalized using the Kolmogorov length  $L_K$  (open squares). The analytic approximation (17) to this spectrum  $\Psi_N$ , (solid line) and its integral  $I_N$ , [(20); dotted line]. The wavenumbers at which the integral reaches 50%–95% of its ultimate value of  $2/15$  are indicated by the solid symbols. The gray shading shows the range that contains 90% of the shear variance.

where  $\hat{k} = k L_K$  is the nondimensional cyclic wavenumber (Fig. 6, solid line). The integral of this approximation is 0.1% larger than  $2/15$ .

The compensated Nasmyth shear spectrum,  $\hat{k}^{-1/3} \Psi_N(\hat{k})/7.89$ , is level at 1 at low wavenumbers, but it rises to a peak of 1.15 at a cyclic wavenumber of 0.018. The compensated rate of strain spectrum does not have a peak. Volk et al. (2002) considered the eighth spectral value erroneous and excluded it from their analytic approximations. However, this spectral point may not be erroneous because the wind tunnel observations by Saddoughi and Veeravalli (1994) indicate that there is a peak in the shear spectrum, although the peak reported by them is slightly smaller (1.08) and at a slightly lower wavenumber of 0.013. Saddoughi and Veeravalli (1994) report a peak in the compensated spectrum for all three velocity components while the compensated along-profile velocity spectrum of PN does not have a peak.

## 2) THE PANCHEV–KESICH MODEL

A three-dimensional spectrum of turbulent velocity was derived by Panchev and Kesich (1969) and this spectrum must be integrated numerically to derive the one-dimensional spectrum of cross-profile velocity fluctuations. The shear spectrum is obtained by multiplying this derived velocity spectrum by  $\hat{\kappa}^2$ , where  $\hat{\kappa}$  is the nondimensional angular wavenumber. An analytic approximation of the Panchev–Kesich shear spectrum, according to Roget et al. (2006), is

$$\Psi_{PK}(\hat{k}) = 11.9 \hat{k}^{0.372} \exp(-90.9 \hat{k}^{1.495}), \quad (18)$$

where  $\hat{k}$  is the cyclic nondimensional wavenumber. This spectrum rises more steeply than  $\hat{k}^{1/3}$  in the inertial subrange,

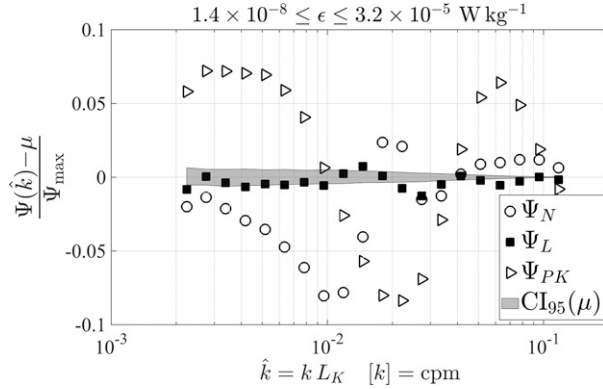


FIG. 7. The differences between the three approximations of the shear spectrum and the bin-averaged spectrum  $\mu$  for each bin, divided by the spectral maximum of  $\Psi_{\max} = 2.32$ . The gray shading is the 95% bootstrap confidence interval for the bin averages. Open circles: the Nasmyth approximation of (17). Filled squares: the new approximation of (13). Open triangles: the Panchev–Kesich approximation of (18).

which is inconsistent with the high Reynolds number wind tunnel measurements by [Saddoughi and Veeravalli \(1994\)](#). The integral of this spectrum is 0.2% larger than 2/15.

### c. Comparison of approximations

The bin-averaged spectrum deviates by up to 8% from the approximations of the Nasmyth and the Panchev–Kesich spectra (Fig. 7, open circles and triangles). The difference between approximations of the shear spectrum and the bin-averaged spectrum are normalized by the spectral peak of  $\Psi_{\max} = 2.32$  to turn the differences into a fraction. The gray shading is the 95% bootstrap confidence interval for the bin averages (minus the bin average itself). Both the Nasmyth and the Panchev–Kesich approximations are well outside of this confidence interval. The new approximation  $\Psi_L$  is mostly within the confidence interval (Fig. 7, filled squares). The approximation of [Wolk et al. \(2002\)](#) (not shown) deviates by about twice as much as the Nasmyth spectrum  $\Psi_N$  of (17) proposed here. The mean absolute deviations of the spectral approximations from the bin-average spectrum are 0.013, 0.06, 0.10, and 0.11, for the new, the Nasmyth, the [Wolk et al. \(2002\)](#), and the Panchev–Kesich approximations, respectively.

The peak of the measured spectrum is 2.3, and thus, a mean absolute deviation of 0.013 is less than 1% of this peak but it is unlikely that the approximation is that reliable. Wavenumbers of  $\hat{k} > 0.15$  are dominated by electronic noise because of the high wavenumber rise of the spectrum (Fig. 5). The electronic noise is nearly fixed with respect to the dimensional wavenumber, but not with respect to the nondimensional wavenumber. The rate of dissipation estimated from the spectra varies by three factors of 10 (Fig. 8) and the majority of the values are between 1 and  $30 \times 10^{-7} \text{ W kg}^{-1}$ . Spectra with high  $\epsilon$  are above the electronic noise at the highest wavenumber considered here (150 cpm) and the highest nondimensional wavenumber is smaller than 0.1. That is, the contribution of electronic noise to high- $\epsilon$  estimates is small. Spectra with very

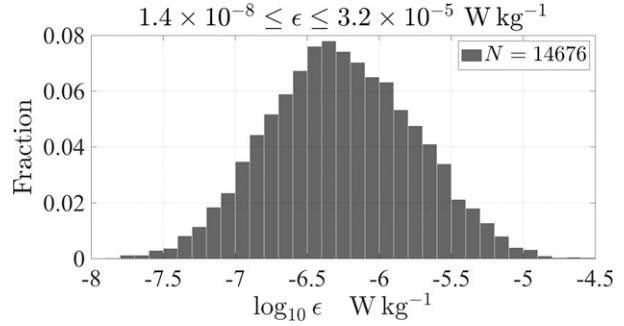


FIG. 8. The frequency distribution of dissipation rates for the nondimensional spectra. The smallest and largest of the 14676  $\epsilon$  values are  $1.4 \times 10^{-8}$  and  $3.2 \times 10^{-5} \text{ W kg}^{-1}$ , respectively.

small  $\epsilon$  are dominated by noise for wavenumbers above 80 cpm and their largest nondimensional wavenumber reaches 0.4. That is, the contribution of electronic noise to these dissipation estimates is not small. The upper edge of the last bin was set to 0.13 in order to reduce the spectral bias due to electronic noise.

The influence of electronic noise was examined by choosing spectra from three different ranges of the rate of dissipation, namely,

$$\begin{aligned} 1.4 \times 10^{-8} < \epsilon &\leq 3.5 \times 10^{-7} \text{ W kg}^{-1}, \\ 3.5 \times 10^{-7} < \epsilon &\leq 1.0 \times 10^{-6} \text{ W kg}^{-1}, \\ 1.0 \times 10^{-6} < \epsilon &\leq 3.2 \times 10^{-5} \text{ W kg}^{-1}, \end{aligned} \quad (19)$$

denoted low, medium, and high, respectively. Nondimensional spectra were calculated using these three ranges and were compared to the spectrum derived from the full range of dissipation rates. The heights of the peaks of the spectra for the low, medium, and high dissipation rates, compared to the spectrum that uses the entire range, were 0.95, 0.98, and 1.05, respectively. A higher peak is compensated by a steeper drop off beyond the peak, because all spectra integrate to almost exactly 2/15. Thus,  $\approx \pm 5\%$  may be a more appropriate measure of the uncertainty of this approximation than is the uncertainty implied by its mean absolute deviation value.

### d. Nondimensional shear spectrum integral

A model spectrum also provides an estimate of the fraction of the shear variance that is resolved by integrating its spectrum up to only a finite wavenumber, such as the approximation in (1). An analytic approximation of the integral of the Nasmyth spectrum is

$$\begin{aligned} I_N(\hat{k}) &= \frac{15}{2} \int_0^{\hat{k}} \Psi_N(\xi) d\xi \approx \tanh(61.5 \hat{k}^{4/3}) \\ &\quad - 18.1 \hat{k}^{4/3} \exp(-52.5 \hat{k}^{4/3}), \end{aligned} \quad (20)$$

which agrees within 1% with a numerical integration of an interpolation of the Nasmyth spectrum. An approximation of the integral of  $\Psi_L$  (13) is

$$I_L(\hat{k}) = \frac{15}{2} \int_0^{\hat{k}} \Psi_L(\xi) d\xi \approx \tanh(65.5\hat{k}^{4/3}) - 19.0\hat{k}^{4/3} \exp(-54.5\hat{k}^{4/3}), \quad (21)$$

which agrees within 2% with the numerical integration of  $\Psi_L$  for wavenumbers larger than  $\hat{k} > 0.026$ —wavenumbers that resolve more than 35% of the shear variance. The ratio of these two approximations is smaller than 1.05 for wavenumbers beyond the peak of the spectrum. Thus, for most practical applications, the dissipation estimates that are corrected for the unresolved variance will differ by less than 5% when using either  $I_N$  or  $I_L$ .

## 5. Discussion

### a. The $N_f^{-7/9}$ dependence of $\sigma_{\ln \Psi}^2$

The dependence of the variance of the logarithm of a shear spectrum,  $\sigma_{\ln \Psi}^2$  [see (8)], on the number of FT segments,  $N_f$ , used to estimate the spectrum, is a natural consequence of the lognormal pdf of a spectrum. The  $N_f^{-7/9}$  power-law dependence of  $\sigma_{\ln \Psi}^2$  can be replicated using synthetically generated spectra with the following steps. A pair of normally distributed sequences,  $X$ , each of length 71 (the typical number of points in a spectrum), is drawn from a random number generator and they are scaled to have a variance of  $\sigma^2 = 2.76$ . The pair is transformed into linear space using  $\Psi = \exp(-\sigma^2/2)\exp(X)$  so that each of the two  $\Psi$  has an expectation of 1, and they are then smoothed with weights [1/4 1/2 1/4] to replicate the effect of a cosine window used in standard spectral estimation. Each  $\Psi$  is multiplied by  $\Psi_L$  (13), to generate a pair of periodograms with an expectation equal to this approximation of the universal shear spectrum. The above steps are repeated  $N_f$  times and averaged to produce a pair of shear spectra. The pair of spectra are saved for later statistical analysis. The above steps are repeated 2000 times, for each value of  $N_f$  ranging from 1 to 100.

The smoothing with the weights of [1/4 1/2 1/4] reduces the variance of the periodograms to  $\sigma^2 = 5/4$  and equal to the empirically derived variance (8) for  $N_f = 1$ . The half variance of the logarithm of the ratio of the two synthetically derived spectra,  $0.5 \times \text{Var}[\ln(\Psi_1/\Psi_2)]$ , agrees closely with the empirically derived variance (Fig. 9, disks and solid line), particularly its  $N_f^{-7/9}$  decrease with increasing  $N_f$ .

The rate of dissipation is proportional to the integral of the shear spectrum. Consequently, the variance of  $\ln \epsilon$  derived from the integral of a shear spectrum must agree with the variance of  $\ln \epsilon$  derived directly from the variance of shear in the spatial domain (as derived in Part I). The agreement is tested by generating 2000 synthetic spectra, using the method described above, that have an expected rate of dissipation of  $\epsilon = 4.7 \times 10^{-7} \text{ W kg}^{-1}$ , which equals the median rate observed in Minas Passage. The rate of dissipation is calculated using the method described in section 2b and the variance of the derived values are computed for  $N_f$  ranging from 1 to 100. The nondimensional averaging length is taken to be  $\hat{L} = L_f N_f / L_K$ , where  $L_f = 0.5 \text{ m}$  is the physical length of a single FT segment. The variance of the thusly calculated dissipation rates agrees closely with the variance of the

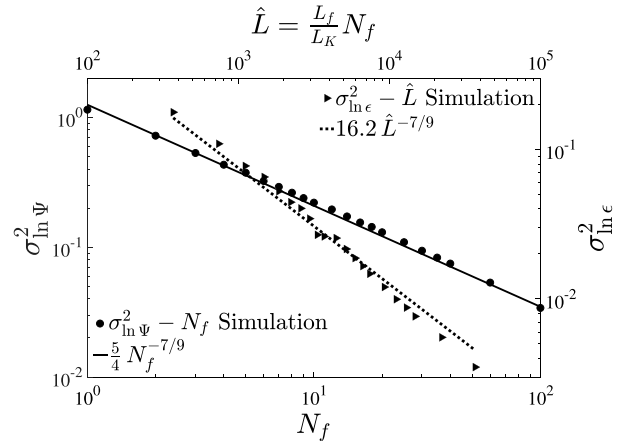


FIG. 9. Left and bottom axes: the variance of the logarithm of a spectrum,  $\sigma_{\ln \Psi}^2$ , derived from a simulation (disks) and its empirical model (8) (black line), vs the number of FT segments,  $N_f$ , used to compute a spectrum. Top and right axes: the variance of the logarithm of  $\epsilon$  derived from the integral of simulated spectra (triangles) and the empirical model of Eq. (11) of Part I (dotted line) vs the length of data,  $\hat{L}$ , used to estimate the spectra.

dissipation rates derived in Part I (Fig. 9, triangles and dotted line). Thus, the statistical uncertainty of the two methods of estimating  $\epsilon$  are equal when identical data lengths are used to make an estimate.

### b. Which spectral approximation is best?

Although the bin average of 14 600 nondimensional spectra has a confidence range that is tight enough to distinguish its departure from the approximations of the Nasmyth and the Panchev–Kesich spectra, the choice of a reference spectrum is not critical in most practical applications. The practical range of  $N_f$  is less than 100. Substituting  $N_f = 100$  in (8) gives a 95% confidence interval of [0.69 1.45], which is far larger than the difference between the bin averages and the approximations of the spectra of Nasmyth and Panchev–Kesich (Fig. 7). That is, any of the three approximations,  $\Psi_L$ ,  $\Psi_N$ , and  $\Psi_{PK}$ , can serve as a reference spectrum for judging the quality of a measured spectrum, as can the approximation proposed by Wolk et al. (2002).

### c. Spectral confidence

The quality of a measured spectrum of shear can be judged by comparing the logarithm of this spectrum against the logarithm of any one of the models of the expectation spectrum. If this difference exceeds  $2.5\sigma_{\ln \Psi}$  then there is a probability of about 1%, or less, that this occurred by chance alone. Such spectral values should be rejected and replaced with an interpolated value, if the anomaly is highly isolated (very narrow banded), and the spectrum should be reintegrated to determine the variance of shear. The anomaly may also be caused by vibrational contamination that was not adequately removed, or may be unremovable.

A broader measure of the quality of a spectrum can be obtained by calculating the standard deviation [or the mean



absolute deviation (MAD)] of the difference of the logarithm of the spectrum and the expectation spectrum, over the range of wavenumbers used for spectral integration. This range will scale approximately with  $\epsilon^{1/4}$  and encompass fewer than  $\sim 10$  spectral values at very low rates of dissipation ( $\sim 10^{-10}$  W kg $^{-1}$ ) and many tens of spectral values for high rates. The STD (or MAD) of this spectral difference has an expectation of  $\sigma_{\ln\Psi}$  (or  $0.80\sigma_{\ln\Psi}$ ). However, the number of spectral values available for this calculation is limited, and the empirical estimate of the STD will have a spread that is larger than the spread of a normal distribution. For a Gaussian process that has a standard deviation of  $\sigma$ , 97.5% of the estimates of the STD of this process are smaller than  $\sigma T_S$ , where

$$T_S = 1 + \sqrt{\frac{2}{N_s}} \quad (22)$$

and  $N_s \geq 5$  is the number of samples drawn from the process. The upper 97.5th percentile for a MAD estimate is  $\sigma T_M$ , where

$$T_M = 0.8 + \sqrt{\frac{1.56}{N_s}}. \quad (23)$$

Therefore, a measure of the quality of a spectrum, over the wavenumber range used to make an  $\epsilon$  estimate is

$$Q_S = \frac{s_{\ln\Psi}}{\sigma_{\ln\Psi}} \frac{1}{T_S}, \quad (24)$$

where  $s_{\ln\Psi}$  is the standard deviation of the  $N_s$  spectral values that were used in the estimation of the  $\epsilon$ . Similarly, if a MAD is preferred, then a measure of the quality of the spectrum is

$$Q_M = \frac{\text{MAD}_{\ln\Psi}}{\sigma_{\ln\Psi}} \frac{1}{T_M}. \quad (25)$$

Both  $Q_S$  and  $Q_M$  are expected to be smaller than 1 for 97.5% of spectra. Some allowance should be made for the uncertainty of  $\sigma_{\ln\Psi}$  and the expectation spectrum, and perhaps  $Q_S$ ,  $Q_M > 1.1$  is a suitable criterion for rejecting a spectrum. Because the pdf of the logarithm of a shear spectrum in normal, it is possible to apply the various  $t$  tests to the spectrum—for example, are two simultaneously measured spectra different?

The measurement uncertainty derived here is not unique to a shear-probe spectrum. It should apply to all sensors that are used to measure shear. Moreover, because a shear spectrum is just a velocity spectrum multiplied by  $(2\pi k)^2$ , the uncertainty also applies to cross-profile velocity measurements, such as those taken with an acoustic sensor. Many sensors cannot resolve the dissipation range of the velocity spectrum. For such sensors, the level of the velocity spectrum in the inertial subrange is often used to estimate the rate of dissipation because, in this range, the spectrum should equal  $A\epsilon^{2/3}k^{-5/2}$ , where  $A = 1/5$  is the one-dimensional cross-profile Kolmogorov constant, when wavenumbers are expressed in units of cpm (Kolmogorov 1941; Pope 2009). Dividing the velocity spectrum by  $Ak^{-5/3}$  and then taking its logarithm produces

estimates of  $\ln\epsilon^{2/3}$  that are normally distributed with a standard deviation of  $\sigma_{\ln\Psi}$ . Averaging these values over a range of wavenumbers reduces its standard deviation by the square root of the number of spectral points used for the average. This reduced value of  $\sigma_{\ln\Psi}$  can then be used to determine the confidence range of the average of  $\ln\epsilon^{2/3}$  and, thus, of  $\epsilon$  itself.

The uncertainty derived here must also apply, at least approximately, to the rate of strain (and the along-profile velocity) spectrum because  $\epsilon$  is also proportional to the variance of the rate of strain. However, the strain spectrum is lower and broader than the shear spectrum, making it unlikely that  $\sigma_{\ln\Psi}$  applies identically to this velocity component.

It should not be surprising that the pdf of a spectrum is lognormal rather than  $\chi^2$  because turbulence shear is not Gaussian normal, which is frequently assumed in spectral analysis. The rate of dissipation is distributed lognormally and it is also proportional to the integral of the shear spectrum. Averaging is proportional to integration. Consequently, the spectral values must also be lognormally distributed.

## 6. Conclusions

The logarithm of the spectrum of turbulent shear has a probability distribution that is Gaussian normal. The variance of a spectral estimate,  $\sigma_{\ln\Psi}^2$ , decreases with increasing number of FT segments that are used to estimate a spectrum, according to (8), and this relationship holds for both the unstratified conditions of a tidal channel (Minas Passage) and for the stratified thermocline (Faroe Bank Channel). The measurement uncertainty appears to be independent of the rate of dissipation  $\epsilon$  and only slightly dependent on the wavenumber of the spectral values. The spectral uncertainty is consistent with the uncertainty of the estimates of the rate of dissipation that are derived directly from the variance of the shear, in the space domain, using the first equality in (1).

The 18.5 km of the data collected in Minas Passage are used to produce a new empirical turbulence shear spectrum based on approximately 14 600 nondimensional spectra each containing 5 m of data. Bin averages of these spectra deviate from the Nasmyth spectrum  $\Psi_N$  [see (17)] and from the Panchev–Kesich spectrum  $\Psi_{PK}$  [see (18)] by up to 8%. The bin average spectrum is well approximated by  $\Psi_L$  [see (13)]. Any one of these three spectra can be used as a reference (or expectation) for a measured spectrum. An approximation of the integral of the  $\Psi_L$  spectrum is given by (21), and does not differ substantially from the approximation of the integral of the Nasmyth spectrum, given by (20). Both  $\Psi_L$  and  $\Psi_N$  rise by a factor of 1.14 above the  $k^{1/3}$  trend of the inertial subrange, at the cyclic nondimensional wavenumbers of 0.013 and 0.018, respectively.

The expected standard deviation of the logarithm of a spectrum can be used to test the equality of two or more spectra, and the deviation of the logarithm of a spectrum from a reference spectrum provides a means to quantify the quality of a spectrum.

*Acknowledgments.* The Nemo data were supplied by Alex Hay of Dalhousie University. Dave Cronkrite and

Evan Cervelli of Rockland Scientific, Inc., and Richard Cheel of Dalhousie deployed and recovered the Nemo float. The Faroe Bank glider data were supplied by Ilker Fer, University of Bergen. I am grateful to Justine MacMillan and the four reviewers who provided many useful comments and suggestions. This work was partially supported by the Canadian Industrial Research Assistance Program under Project 940486.

*Data availability statement.* All data are available from the author.

## REFERENCES

- Fer, I., A. K. Peterson, and J. E. Ullgren, 2014: Microstructure measurements from an underwater glider in the turbulent Faroe Bank Channel overflow. *J. Atmos. Oceanic Technol.*, **31**, 1128–1150, <https://doi.org/10.1175/JTECH-D-13-00221.1>.
- Goodman, L., E. R. Levine, and R. G. Lueck, 2006: On measuring the terms of the turbulent kinetic energy budget from an AUV. *J. Atmos. Oceanic Technol.*, **23**, 977–990, <https://doi.org/10.1175/JTECH1889.1>.
- Grant, H. L., R. W. Stewart, and A. Moilliet, 1962: Turbulence spectra from a tidal channel. *J. Fluid Mech.*, **12**, 241–263, <https://doi.org/10.1017/S002211206200018X>.
- Kolmogorov, A. N., 1941: Local structure of turbulence in an incompressible fluid at very high Reynolds number. *Dokl. Akad. Nauk SSSR*, **4**, 299–303.
- Kraichnan, R. H., 1959: The structure of isotropic turbulence at very high Reynolds numbers. *J. Fluid Mech.*, **5**, 497–543, <https://doi.org/10.1017/S0022112059000362>.
- Lueck, R. G., 2022: The statistics of oceanic turbulence measurements. Part I: Shear variance and dissipation rates. *J. Atmos. Oceanic Technol.*, <https://doi.org/10.1175/JTECH-D-21-0051.1>, in press.
- Nasmyth, P. W., 1970: Ocean turbulence. Ph.D. thesis, University of British Columbia, 69 pp.
- Oakey, N. S., 1982: Determination of the rate of dissipation of turbulent kinetic energy from simultaneous temperature and velocity shear microstructure measurements. *J. Phys. Oceanogr.*, **12**, 256–271, [https://doi.org/10.1175/1520-0485\(1982\)012<0256:D0TROT>2.0.CO;2](https://doi.org/10.1175/1520-0485(1982)012<0256:D0TROT>2.0.CO;2).
- Panchev, S., and D. Kesich, 1969: Energy spectrum of isotropic turbulence at large wavenumbers. *C. R. Acad. Bulg. Sci.*, **22**, 627–630.
- Pope, S. B., 2009: *Turbulent Flows*. Cambridge University Press, 771 pp.
- Roget, E., I. Lozovsky, X. Sanchez-Martin, and M. Figueroa, 2006: Microstructure measurements in natural waters: Methodology and applications. *Prog. Oceanogr.*, **70**, 126–148, <https://doi.org/10.1016/j.pocean.2006.07.003>.
- Saddoughi, S. G., and S. V. Veeravalli, 1994: Local isotropy in turbulent boundary layers at high Reynolds number. *J. Fluid Mech.*, **268**, 333–372, <https://doi.org/10.1017/S0022112094001370>.
- Sreenivasan, K. R., 1995: On the universality of the Kolmogorov constant. *Phys. Fluids*, **7**, 2778–2784, <https://doi.org/10.1063/1.868656>.
- Taylor, G., 1935: Statistical theory of turbulence. *Proc. Roy. Soc.*, **151A**, 421–444, <https://doi.org/10.1098/rspa.1935.0158>.
- Wolk, F., H. Yamazaki, L. Seuront, and R. G. Lueck, 2002: A new free-fall profiler for measuring biophysical microstructure. *J. Atmos. Oceanic Technol.*, **19**, 780–793, [https://doi.org/10.1175/1520-0426\(2002\)019<0780:ANFFPF>2.0.CO;2](https://doi.org/10.1175/1520-0426(2002)019<0780:ANFFPF>2.0.CO;2).